Nonlinear hydrodynamic waves: Effects of the equation of state

N. M. Bulgakova and I. M. Burakov
Institute of Thermophysics SB RAS, prosp. Lavrentyev 1, 630090 Novosibirsk, Russia
(Received 28 January 2004; published 13 September 2004)

The problem of the decay of an initial discontinuity (the Riemann problem) is studied for a substance with abnormal properties when the rarefaction waves get a shock form, whereas the compression waves become nonsharp with the width proportional to the distance traveled. Such a situation is inherent to matter in a near-critical thermodynamic state and is also met in many other physical systems. The behavior of pressure jumps is compared for the van der Waals equation of state and for its more realistic three-parametric modification. It is shown that the evolution of the rarefaction and compression waves is strongly dependent on the value of the fundamental gasdynamic derivative determined by the equation of state. We demonstrate that for some substances with abnormal properties both rarefaction and compression waves can keep a shocklike form for a long period of time after discontinuity decay.

DOI: 10.1103/PhysRevE.70.036303 PACS number(s): 47.40.−x, 47.35.+i, 51.30.+i

I. INTRODUCTION

Recently it has been shown that, under ultrashort-pulse laser ablation of solids, the rarefaction shock wave (RSW) can be formed in laser-induced plumes [1,2]. An intriguing picture of the formation of a compressed layer in the ablation products expanding in a vacuum has been revealed after RSW reflection from a nonvaporized target surface. There is a widespread erroneous opinion that RSW's may be generated only under exotic conditions such as a substance in a state near the thermodynamic critical point. However, the RSW appears to be a fairly general phenomenon which it is possible to observe in expanding and stationary plasmas [3–5], particularly in magnetized [6,7] and optically thin radiative plasma [8], in a nonequilibrium vibrationally excited gas [9], and in binary gas mixtures [10]. It has been speculated that the RSW may be observed under implosions of internal confinement fusion pellet materials [11] and in stellar envelopes [2]. A fascinating picture is formed in the transonic flows of inviscid fluids with regions of negative and positive nonlinearities [12,13]. It has been shown that in spherical geometry the RSW effects can be even more pronounced than in planar geometry [2,14,15]. It has been suggested that the effects related to the RSW's may prove to be important for practical use [16,17] in postponing the phenomenon of choking of real gas flows in pipes [16] and improving organic Rankine cycle engines [17] due to weakening shock-wave impacts. Thus, a new field of hydrodynamics of the rarefaction shock waves, suggesting their reflection from solid surfaces, interference between them and with the compression waves, their transformation from a shock to a widening structure, and vice versa, has invited a large body of investigation.

The possibility of RSW formation in the vicinity of the "liquid-vapor" critical point was first predicted by Bethe [18] and Zeldovich [19] and demonstrated experimentally for the first time in 1980 by Borisov *et al.* [20,21]. Let us first recall that the RSW's are formed in a matter whose adiabats have a part with negative curvature that fulfills the condition $(\partial^2 p/\partial v^2)_S<0$ or $\Gamma=(v^4/2a)(\partial^2 p/\partial v^2)_S<0$ (p, v, a, and S are the pressure, specific volume, sound speed, and entropy, respectively, and Γ is the fundamental gas-dynamic derivative introduced by Thompson [22]). So-called Bethe-Zeldovich-Thompson (BZT) fluids have $\Gamma<0$ (negative nonlinearity), contrary to classic fluids with positive nonlinearity $\Gamma>0$ (e.g., perfect gas). When the condition $\Gamma<0$ is fulfilled, the velocity of the rarefaction wave becomes supersonic (with respect to the sound speed in the unperturbed medium [21]), leading to the formation of a discontinuity in the medium parameters which keeps its steepness during evolution—i.e., to the RSW formation by definition given in Ref. [19]. At the same time, the compression waves in BZT fluids become nonsharp with the width proportional to the distance the wave has traveled. Analytically the evolution of a single rarefaction shock wave has been considered in Ref. [21]. One-dimensional numerical studies of the formation and evolution of rarefaction and compressive waves in BZT fluids with the van der Waals equation of state (EOS) have been performed in Refs. [11,12,23] for the shock-tube problem, particularly with reflection from end walls [23]. Numerous classical and nonclassical effects have been revealed in such a simple geometry, like composite shocks and splitting waves. It has been shown that negative nonlinearity can be realized for materials with different EOS [24]. Recently [15] we have shown that, for the three-parametric modification of the van der Waals EOS [25,26] which accurately describes a wide variety of substances, the RSW behaves differently as compared to the case with the classic van der Waals EOS [2], which is worthy of detailed study.

In this paper we present the results of numerical modeling of the shock-tube problem for fluids with the van der Waals EOS and its three-parametric modification in the adiabatic flow case. For these two sorts of fluid, the formation and evolution of rarefaction and compression waves are compared for the cases with $\Gamma<0$ and $\Gamma>0$. The effect of the value of the fundamental gas-dynamic derivative on the wave dynamics is discussed.

II. MODEL

We consider a shock tube of a finite length divided by a membrane into two equal parts with different pressures of a

substance filling the tube. In both parts the substance is in a state near the thermodynamic critical point but outside of the two-phase region. After instantaneously breaking the membrane, waves of compression and rarefaction are formed in the substance and we study, in a one-dimensional approximation, their evolution, reflection from end walls, and interference. The modeling set of equations includes the compressible nondissipative conservation equations for mass, momentum, and energy (the Euler equations) [2,11,12]:

$$\frac{\partial \rho}{\partial t} + \frac{\partial}{\partial x}(\rho u) = 0,$$

$$\frac{\partial u}{\partial t} + u\frac{\partial u}{\partial x} = -\frac{1}{\rho}\frac{\partial p}{\partial x},$$

$$\frac{\partial}{\partial t}\left(e + \frac{u^2}{2}\right) + u\frac{\partial}{\partial x}\left(e + \frac{u^2}{2}\right) + \frac{1}{\rho}\frac{\partial}{\partial x}(pu) = 0. \qquad (1)$$

Here x is the distance along the shock tube, ρ is the mass density, u is the velocity, and e is the internal energy. The system of equations is supplemented by either the van der Waals EOS (referred to below as primary)

$$p = \frac{RT}{v - b} - \frac{a}{v^2} \qquad (2)$$

or the generalized van der Waals EOS proposed by Martynyuk *et al.* [25,26]:

$$p = \frac{RT}{v - b_1} - \frac{a_1}{v^n}, \qquad (3)$$

where T and R are the temperature and universal gas constant, respectively. The coefficients a and b are equal to $9RT_c v_c/8$ and $v_c/3$, respectively, with the index c denoting the critical parameters. The values of the coefficients n, a_1, and b_1 are determined by the critical factor z_c:

$$z_c = \frac{p_c v_c}{RT_c} = \frac{n^2 - 1}{4n}. \qquad (4)$$

From Eq. (4) it follows that $n = 2z_c + \sqrt{4z_c^2 + 1}$ and the parameters a_1 and b_1 are written as $a_1 = \alpha RT_c v_c^{n-1}$ and $b_1 = \beta v_c$ where the coefficients $\alpha = (n+1)^2/4n$ and $\beta = (n-1)/(n+1)$ are dependent only on z_c and differ from $9/8$ and $1/3$ peculiar to the primary van der Waals EOS.

A caloric equation corresponding to the particular EOS closes the system of equations (1)–(4). The system is solved numerically in the Lagrangian coordinates in dimensionless form with p_c, v_c, T_c, L, and $u_c = \sqrt{T_c/M}$ as the characteristic parameters (L is the shock-tube length and M is the molecular mass of the substance). The shock tube is divided into 2000 numerical cells, and the explicit difference scheme is used in which the velocities are calculated at the cell boundaries whereas the other parameters are calculated in the cell centers. This allows us to use only one boundary condition $u|_{x=0} = u|_{x=L} = 0$ at the end walls. The scheme which is first order in time and second order in space has been tested by solving the problem of the decay of an initial discontinuity for the conditions reported in Ref. [12].

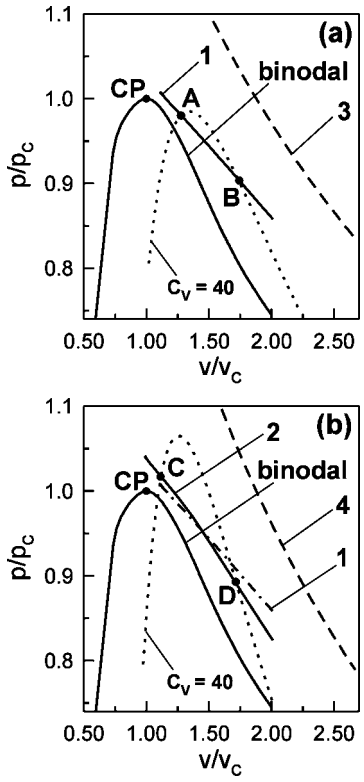

FIG. 1. p-v phase diagrams: (a) corresponds to the generalized van der Waals EOS [25,26] and (b) is for the primary van der Waals EOS. The critical point (CP) is shown in the top of binodal. Abnormal regions for $c_v/R = 40$ are located under the dotted lines where $(\partial^2 p/\partial v^2)_S = 0$. A set of comparative simulations was performed for the abnormal adiabats 1 and 2 and for the normal adiabats 3 and 4. To compare the adiabat slopes, adiabat 1 is given in (b) by the dash-dotted line.

The initial conditions were chosen on the basis of analysis of the p-v phase diagrams shown in Fig. 1 for the generalized (a) and primary (b) van der Waals EOS. The boundary of the region with negative nonlinearity, $\Gamma < 0$, is found by setting $(\partial^2 p/\partial v^2)_S = 0$, which gives the following expression for the primary van der Waals EOS, assuming the temperature-independent specific heat at constant volume $\tilde{c}_v = c_v/R$ [24]:

$$\tilde{p} = \frac{1}{\tilde{v}^2}\left(\frac{2(3\tilde{v} - 1)^2}{\tilde{v}^2(\tilde{c}_v^{-1} + 1)(\tilde{c}_v^{-1} + 2)} - 3\right). \qquad (5)$$

Here the pressure and specific volume are normalized to the corresponding critical parameters. For the generalized van der Waals EOS, the analogous expression takes the form

$$\tilde{p} = \frac{\alpha}{z_c \tilde{v}^n}\left(\frac{n(n+1)}{\tilde{v}^2}\frac{(\tilde{v} - \beta)^2}{(\tilde{c}_v^{-1} + 1)(\tilde{c}_v^{-1} + 2)} - 1\right). \qquad (6)$$

In the vicinity of the "liquid-vapor" critical point, conditions (5) and (6) are fulfilled for substances with a reasonably high value of $\tilde{c}_v$. It is known that, as a substance approaches its critical temperature, c_v increases, tending to infinity by a near-logarithmic law that is true for both $T_c < 0$ and $T_c > 0$ [27]. So it is expected that negative nonlinearity is an inher-

TABLE I. The initial conditions used in the present calculations. Indices l and r refer to the left and right parts of the shock tube.

Variant	$\tilde{n}_l$	$\tilde{T}_l$	$\tilde{p}_l$	$\tilde{n}_r$	$\tilde{T}_r$	$\tilde{p}_r$
(1)	0.797	0.998	0.983	0.571	0.989	0.902
(2)	0.904	1.006	1.02	0.575	0.991	0.888
(3)	1.1	1.05	1.35	0.525	1.027	0.994
(4)	1.1	1.1	1.465	0.524	1.069	0.987

ent feature of a wide variety of substances in a near-critical-point state. Results will be presented below for $\tilde{c}_v=40$. In Fig. 1, the lines with $\Gamma=0$ are shown by dotted curves for the chosen value of $\tilde{c}_v$, so that $\Gamma<0$ under these curves. We solve the problem for several sets of the initial conditions corresponding to both abnormal (1 and 2) and normal (3 and 4) adiabats. For the generalized van der Waals EOS, the critical factor z_c is taken to be equal to 0.2 (for the majority of substances z_c lies in the range 0.1–0.3 [28,29]), so that $n=1.477$, $\alpha=1.0385$, and $\beta=0.1926$. At the initial time moment the particle densities (n_l, n_r) and temperatures (T_l, T_r) are distributed uniformly within the volume of the left (index l) and right (index r) parts of the shock tube, so that $p_l > p_r$. The values of the initial parameters are given in Table I. The numbers of variants for the calculations correspond to adiabat numbers in Fig. 1. In variants 1 and 2, fluids evolve along the abnormal portions of the adiabats *AB* and *CD*, respectively.

III. RESULTS AND DISCUSSION

The results of the modeling are given in Figs. 2–6. Figures 2 and 3 present the comparison of the pressure and density profiles for the cases of generalized (a) and primary (b) van der Waals EOS (variants 1 and 2, according to Table I). The upper graphs correspond to the time moments $t/\tau=1$ (a) and 0.5 (b) $(\tau=L/\sqrt{T_c/M})$ counted from the decay start. As, initially, pressure was higher in the left part of the tube, the rarefaction wave (having the shock form) is moving to the left. The compression wave is moving to the right wall and its slope is close to that of the RSW for both EOS (directions of wave propagation are indicated by arrows). The vertical dashed lines show the location of initial discontinuity (contact surface). In the Riemann problem, the contact surface is usually seen as a jump in the density profiles (Fig. 3) which is small in the cases presented but can be quite large as, e.g., in Ref. [11] depending on the initial conditions. The lower graphs in Figs. 2 and 3 show the pressure and density profiles formed at the time moments when both waves have reflected twice from the walls. It corresponds to $t/\tau=9.6$ for the generalized EOS and 5.7 for the primary van der Waals EOS. At these time moments, the RSW's are moving again to the left and the compression waves are moving to the right walls. The difference in time of passing the same distance by the waves is explained by the difference in the slopes of the abnormal portions of the corresponding adiabats [see Fig. 1(b) where both abnormal adiabats are given for comparison], characterizing the speed of sound and, hence, the wave velocities. A noticeable difference has become apparent between the waves in the fluids with the different EOS. For the primary van der Waals EOS, the waves

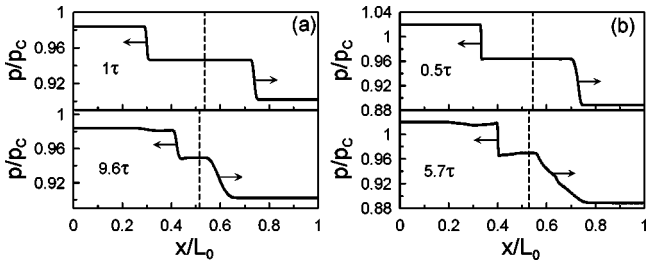

FIG. 2. The pressure profiles in the shock tube for (a) the generalized van der Waals EOS and (b) the primary van der Waals EOS for the evolution along the abnormal adiabats 1 and 2, respectively (Fig. 1). The initial conditions are given in Table I. Coordinates $x/L=0$ and 1 correspond to the positions of the end walls. The time moments are indicated in the figures $(\tau=L/\sqrt{T_c/M})$. Directions of wave propagation are indicated by arrows. The upper graphs are given for the time moments before wave reflection from the shock-tube end walls and the lower graphs correspond to the time moments after double reflection of the waves from the endwalls.

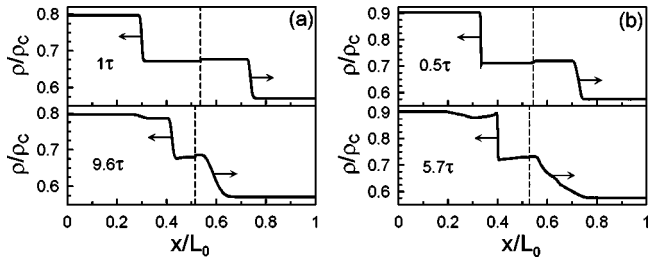

FIG. 3. The density profiles corresponding to Fig. 2.

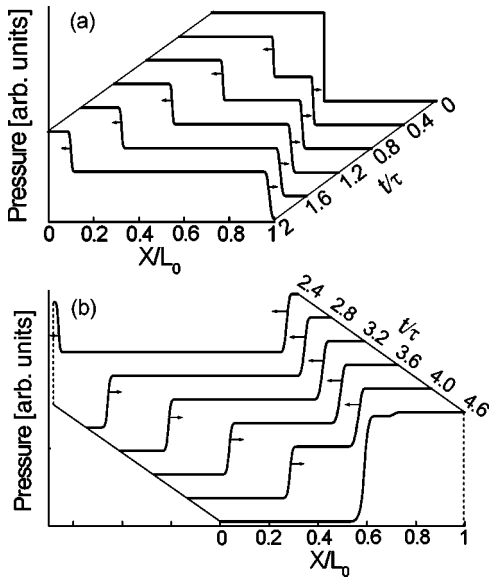

FIG. 4. The successive stages of the decay of the initial discontinuity showing the formation of the rarefaction and compression waves, their propagation in the tube, reflection from the end wall, and their first encounter after reflection for the generalized van der Waals EOS (evolution along the abnormal adiabat 1, Fig. 1).

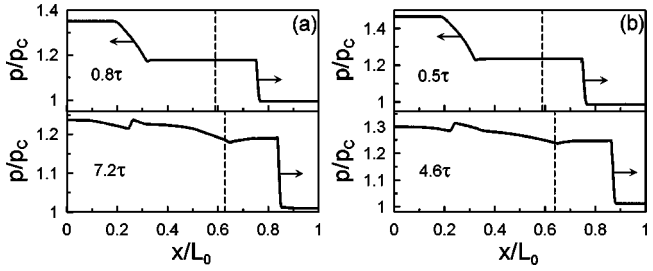

FIG. 5. The same as in Fig. 2 but for the evolution of fluids along the normal adiabats 3 and 4 (Fig. 1).

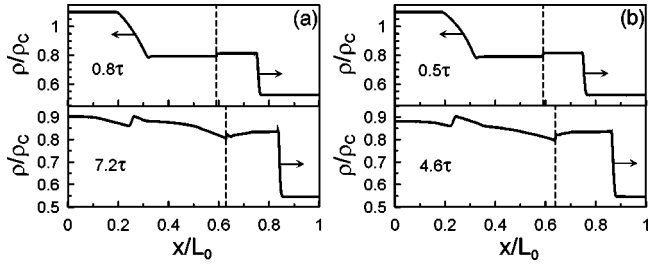

FIG. 6. The density profiles corresponding to Fig. 5.

behave according to the prediction [19,30]: the rarefaction wave is a shock wave whereas the front width of the compression wave increases with distance traveled. In the case of the generalized van der Waals EOS, the rarefaction wave is sharp enough to be called a shock wave, while the compression wave is also steep, distinctly steeper than that for the primary van der Waals EOS (compare the lower graphs in Figs. 2 and 3). It should be emphasized that this is not a result of reflection of the waves from the endwalls. The same picture was also obtained in one-dimensional (1D) modeling of the initial discontinuity decay in the "infinite" shock tube.

Figure 4 presents the successive stages of the decay of the initial discontinuity with the formation of the rarefaction and compression waves, their propagation in the tube, reflection from the end wall, and their first encounter after reflection for the generalized van der Waals EOS (variant 1, according to Table I). The picture is divided into two parts so that the subsequent profiles do not overlap the preceding ones. After decay of the initial discontinuity shown at time moment $t/\tau=0$, the rarefaction and compression waves are formed and move to the end walls as shown by the arrows [Fig. 4(a)]. The compression wave is the first to reach the end wall, reflects and starts to move back, while the RSW is still on its way to the respective end wall [$t/\tau=2.4$ in Fig. 4(b)]. However, it does not contradict the supersonic nature of the RSW as defined in Sec. I. After RSW reflection from the end wall, the waves move towards each other ($t/\tau=2.8-4.0$) until they meet at $t/\tau=4.6$ [Fig. 4(b)] and the pressure profile becomes converse to that for $t/\tau=0$ [Fig. 4(a)] which can be considered as the formation of a new discontinuity. As a result of the interaction of the waves, small perturbations can occur as seen in the profile for $t/\tau=4.6$ and in Fig. 2(a), lower graph. After decay of the discontinuity formed, the picture of wave formation, their propagation to the end walls and reflection is repeated. However, both the rarefaction and compression waves keep the forms of the steep jumps [Fig. 2(a), lower graph].

The nonlinear wave behavior demonstrated above is inherent only for abnormal (BZT) fluids with $\Gamma<0$. If a fluid is evolving through the regions with both normal ($\Gamma>0$) and abnormal ($\Gamma<0$) thermodynamic properties, the picture of both rarefaction and compression waves is more complicated, exhibiting wave splitting to the shock and dispersed parts [12,13]. In the case of a fluid with positive nonlinearity, the rarefaction and compression waves behave classically, regardless of the EOS form under consideration. Modeling was performed for adiabats 3 and 4, which are located well above the abnormal zones (see Fig. 1 and corresponding variants 3 and 4 in Table I). The pressure and density profiles for both the generalized [Figs. 5(a) and 6(a) and primary [Figs. 5(b) and 6(b)] van der Waals EOS are very similar for equal distances traveled, though they are presented for different time moments. As discussed above, this results from the difference in the slopes of the corresponding adiabats for the different EOS. The upper graphs correspond to the time moments $t/\tau=0.8$ (a) and 0.5 (b) when the waves have not yet reached the end walls after the decay start. One can see that the compression waves are classical shock waves and the rarefaction waves are already wide and smooth. The lower graphs in Figs. 5 and 6 are given for the time moments of 7.2 (a) and 4.6 (b)—that is, after double wave reflection from the end walls. The dynamics of wave propagation is very similar for both EOS. After double reflection from the end walls, the rarefaction waves are fully degraded. Note that, in the BZT fluid for the same distance traveled, the compression wave is still steep [Fig. 2(a), lower graph] or sufficiently narrow [Fig. 2(b), lower graph].

Analyzing Figs. 1–6, one can point out the following.

(a) In fluids with the generalized van der Waals EOS, the rarefaction and compression waves are traveling slower as compared to the primary van der Waals EOS. This difference results from different slopes of the corresponding adiabats in the regions with the abnormal properties demonstrated in Fig. 1(b) (lines 1 and 2).

(b) The most intriguing feature is the small difference between the rarefaction and compression waves for the case of the BZT fluid described by the generalized van der Waals EOS [Fig. 2(a), lower graph, and Fig. 4]. Both the rarefaction and compression waves show the features of shock, though slight spreading is observed even for the RSW. For the BZT fluid with the primary van der Waals EOS [Fig. 2(b)], the RSW keeps sharp while the compression wave is evidently spreading, as was observed in numerous calculations (e.g., [11–13]).

A question arises about the reasons for the similar behavior of rarefaction and compression waves for the BZT fluid with the generalized van der Waals EOS. The answer is in the value of the fundamental gasdynamic derivative which characterizes the convexity of the corresponding adiabat. The calculations show that the modulus of the maximum negative value of $(\partial^2 p/\partial v^2)_S$ in adiabat 1 is about 100 times less as compared to that for adiabat 2 (though it is not evident from Fig. 1). That is, adiabat 1 is much closer to a straight line than adiabat 2. Thus, the factor determining the forms of the rarefaction and compression waves in fluids with abnormal

properties is the extreme value of the fundamental gasdynamic derivative reached in the corresponding portion of the adiabat governed by the EOS. It is necessary to stress that the modified van der Waals EOS [Eq. (3)] is realistic, describing, for example, a wide variety of liquid metals [25,26,29]. It can thus be speculated that there exists a certain sort of fluid whose state is described by an EOS providing an adiabat very close to a straight line within the abnormal region [that is, $(\partial^2 p/\partial v^2)_S \cong 0$]. Most likely both the rarefaction and compression waves will be neither shocks nor spreading structures but will behave similarly to each other for a long time after their formation until the mentioned fluid is in the region of the abnormal properties.

IV. CONCLUSIONS

We have carried out a comparative study of the decay of an initial discontinuity for BZT fluids with two different EOS. The evolution of the rarefaction and compression waves is shown to be strongly dependent on the value of the fundamental gasdynamic derivative determined by the EOS. It is demonstrated that for some substances with abnormal properties both the rarefaction and compression waves can keep their forms close to the shock for a long period of time after discontinuity decay. Such behavior may be expected for many substances with a reasonably high specific heat at constant volume, the condition implying many internal degrees of freedom of substance molecules. On the other hand, in a near-critical-point state, the c_v value increases dramatically in any substances though this requires a definite time to relax. With fast processes like pulsed laser ablation, when c_v relaxation is open to question [1,2], direct cluster emission and clustering in the gas phase [31] can lead to negative nonlinearity development. Whenever possible, the RSW passing through the ablation plume should break off the clustering process. This can be a way to produce clusters with predetermined size distribution.

This study opens up a broad spectrum of new problems concerning BZT fluids which suggests investigations of the evolution of rarefaction and compression waves, including reflection from solid surfaces, their interference and transformation from a shock to a widening structure, and vice versa. Some examples of such studies are under way.

ACKNOWLEDGMENTS

The authors wish to thank A.V. Bulgakov, E.E.B. Campbell, and D. Swindell for valuable discussions. The work was supported by the Russian Foundation for Basic Research (Grants Nos. 02-03-32221 and 03-03-06018) and by a grant of the RF President for support of Leading Scientific Schools No. 910.2003.1.

[1] N.M. Bulgakova, Phys. Rev. E **60**, R3498 (1999).
[2] N.M. Bulgakova, I.M. Bourakov, and N.A. Bulgakova, Phys. Rev. E **63**, 046311 (2001).
[3] B. Bezzerides, D.F. Forslung, and E.L. Lindman, Phys. Fluids **21**, 2179 (1978).
[4] D. Diebold, N. Hershkovitz, and S. Eliezer, Phys. Fluids **30**, 3308 (1987).
[5] D.S. Dorozhkina and V.E. Semenov, Plasma Phys. Rep. **24**, 297 (1998).
[6] M.B. Isichenko and K.V. Chukbar, JETP Lett. **39**, 225 (1984).
[7] R.A. Glatman, Sov. Phys. Tech. Phys. **20**, 1526 (1975).
[8] D.Kh. Morozov and M. Pekker, Phys. Rev. E **64**, 016416 (2001).
[9] E.Ya. Kogan and N.E. Molevich, Acoust. Phys. **39**, 505 (1993).
[10] R.A. Glatman, Sov. Phys. Tech. Phys. **20**, 537 (1975).
[11] J.W. Bates and D.C. Montgomery, Phys. Fluids **11**, 462 (1999).
[12] A.A. Borisov and G.A. Khabakhpashev, J. Appl. Mech. Tech. Phys. **23**, 115 (1982).
[13] D. Chandrasekar and Ph. Prasad, Phys. Fluids A **3**, 427 (1991).
[14] D. Mitrovich, Phys. Fluids **24**, 2159 (1981).
[15] N.M. Bulgakova, A.V. Bulgakov, I.M. Bourakov, and N.A. Bulgakova, Appl. Surf. Sci. **197-198**, 96 (2002).
[16] D. Stojkovic, V.D. Djordjevic, and P.S. Cvijanovic, Int. J. Heat Fluid Flow **22**, 480 (2001).
[17] B.P. Brown and B.M. Argrow, J. Propul. Power **16**, 1118 (2000).
[18] H.A. Bethe, Office of Scientific Research and Development, Report OSRD No. 545, 1942.
[19] J. Zeldovich, Zh. Eksp. Teor. Fiz. **16**, 363 (1946).
[20] Al.A. Borisov, A.A. Borisov, S.S. Kutateladze, and V.E. Nakoryakov, JETP Lett. **31**, 585 (1980).
[21] A.A. Borisov, Al.A. Borisov, S.S. Kutateladze, and V.E. Nakoryakov, J. Fluid Mech. **126**, 59 (1983).
[22] P.A. Thompson, Phys. Fluids **14**, 1843 (1971).
[23] B.M. Argrow, Shock Waves **6**, 241 (1996).
[24] P.A. Thompson and K.S. Lambrakis, J. Fluid Mech. **60**, 187 (1973).
[25] M.M. Martynyuk and R. Balasubramanian, Int. J. Thermophys. **16**, 533 (1995).
[26] M.M. Martynyuk and P.A. Tamanga, High Temp. - High Press. **31**, 561 (1999).
[27] M.A. Anisimov, Usp. Fiz. Nauk **114**, 249 (1974) [Sov. Phys. Usp. **17**, 722 (1975)].
[28] *Handbook of Physical Quantities*, edited by I.S. Grigoryev, E.Z. Meilikhov, and A.A. Radzig (CRC Press, Boca Raton, 1996).
[29] M.M. Martynyuk, Russ. J. Phys. Chem. **72**, 13 (1998).
[30] Ya. Zeldovich and Yu.P. Raizer, *Physics of Shock Waves and High Temperature Hydrodynamic Phenomena* (Academic, New York, 1996).
[31] A.V. Bulgakov, I. Ozerov, and W. Marine, Thin Solid Films **453-454**, 557 (2004).